Development and characterisation of solvent-borne thermally cured cross-linked TiO_2 reinforced Polyceramic coatings for long service-life on industrial metal substrates

O. Tan, O. Çimen, P. Yolcu, B. Çiçek

Polyceramic coatings exhibit the properties of both polymer and ceramic coatings together, such as flexibility and pencil hardness. These coatings are intended to reduce the loss of capital, labour, and energy to achieve industry-required performance under different operating conditions, with long corrosion resistant service life. In this study, two-component polyceramic coatings with a TiO_2 reinforced formula were produced and applied to two different metal surfaces, Sandblasted Aluminium 1050 plate and SAE 304 Stainless Steel sheet, in order to examine the mechanical, physical and chemical properties of the coatings. In addition, the polyceramic coatings were able to form a film on polypropylene plate and SA-66 Glass plate under curing conditions adjusted according to the substrate material, due to their very low surface energy. Resin-compatible solvents, TiO_2 filler, carbon black pigment, resins and a crosslinker added according to the NCO/OH ratio were used in the production of the coatings. Experiments for coating metal substrates were carried out at curing temperatures between 120 and 180 °C, and at curing times between 60 and 120 minutes. In this study, coating formulations were investigated by SEM, EDS, FTIR, and TGA analysis. The coatings showed 8H pencil hardness, 5B level high adhesion to the metal surfaces, high flexibility with 180° mandrel bending, hydrophobicity, and high corrosion resistance in a salt fog test carried out with 5% salt solution at 35 °C in for 700 hours, according to ASTM D3363, ASTM D3359, ASTM D522 and ASTM B117 standards.

KEYWORDS: POLYCERAMIC COATINGS, HIGH CORROSION RESISTANCE, TWO-COMPONENT COATINGS, HIGH ABRASION RESISTANCE, METAL.

INTRODUCTION

Ceramic coatings are extensively studied and used for applications in materials science and related fields, due to a variety of advantageous properties such as high hardness values, ranging from 6H to 9H [1-3], as well as high temperature resistance [4], modulus of elasticity, thermal shock resistance [5] and abundance in nature [6]. Notwithstanding, ceramic coatings have limited use due to their high brittleness and inadequate predictability of material failure. [7]. On the other hand, polymeric coatings are widely used for industrial applications requiring high ductility, elasticity, and high corrosion resistance [8]. However, the utilization of polymer coatings is limited by their poor thermal behaviour [9,10], poor scratch resistance [11] and

Oğuz Tan
Functional Coatings Department, Gizem Frit and Ceramic Glaze San. Tic., Sakarya, Metallurgical and Materials Engineering Department, Yildiz Technical University, İstanbul, Turkey
Turkey. oguz.tan.t@gmail.com

Oğuzhan Çimen, Pınar Yolcu
Gizem Frit R&D Center, Functional Coatings Department

Dr. Buğra Çiçek
Metallurgical and Materials Engineering Department - Yildiz Technical University, Istanbul, Turkey

susceptibility to chemical attacks such as by denatured alcohol, lacquer thinner, mineral spirits, and methyl ethyl ketone ($CH_3CCH_2CH_3$) [12].

Polyceramic coatings, a solvent-containing precursor fluid layer, are a type of physical coating formed on various surface types such as metals, polymers and glasses. These can be applied by spraying, brushing or wiping, followed by thermal curing conditions appropriate to the remaining components of the precursor liquid after evaporation of the solvents [13]. Polyceramic coatings are hybrid systems; the organic components allow tailoring of hydrophobicity, flexibility, functional compatibility and toughness, whereas the inorganic components improve scratch resistance, density, abrasion resistance, high-temperature resistance, durability, and adhesion ability to the metal surface due to the formation of strong covalent Metal–O–Metal bonds [14-16]. Thus, polyceramic coatings have numerous advantages over either polymeric or ceramic coatings based on their properties and preparation process. The high temperature and abrasion resistance properties of polyceramic coatings are provided by the SiO_2 ceramic structure which forms the backbone of the polyceramic resin. Physical and chemical properties such as high flexibility and corrosion resistance are provided by the polymer chain structure. In addition, functional properties such as hydrophobicity, oleophobicity, and easy cleanability can be provided by modification of the reactive ends connected to the backbone of the polymer chain [17]. In addition to all these features, two-component polyceramic coatings have a blocked-isocyanate cross-linker as a second component, with cross-linked structures providing better mechanical properties than linear polymers. Blocked-isocyanate was added according to the NCO/OH ratio in order to ensure crosslinking with the acrylic resin and polyceramic resin [18]. The NCO in the blocked-isocyanate is released at the curing temperature (120-180 °C) and reacts with the hydroxyl-terminated component of the system to form a rigid, cross-linked polymer structure [19-21]. The polyceramic coating mechanism is based on the difference in surface tension between the coating and the substrate due to the decrease in surface energy provided by the presence of the reactive groups, SiO_2 polyceramic backbone and TiO_2 addition [22-25]. The surface energies of the substrates to which the coatings were applied in the experiments are shown in Table 1 [25-27]. In addition to the surface tension difference, another mechanism to ensure adhesion to the metal surfaces is based on covalent bonding of the silicon in the polyceramic resin with hydroxyl groups on the metal substrates, as illustrated schematically in Figure 1 [27-30], and acrylic resin in the coating formulation with the hydroxyl group in the metal substrates, as described in the literature [31,32]. This study aims to develop an overarching framework to increase corrosion resistance and provide long service-life for industrial metal surfaces prone to degradation due to high temperatures, harsh chemicals, humid environments and UV rays [33,34]. With this aim in mind, in this paper we present new solutions to provide longevity to metal parts under different climatic conditions thanks to the wide working temperature and chemical resistance range of these coatings. Furthermore, polyceramic coatings can be applied to parts with complex shapes by spraying, and avoid incompatibility arising from the usage of metals working together with separate coatings. All of these advantages make this technology particularly valuable in various sectors such as defense, automotive, sports equipment, and accessories such as eyeglasses and watches. This study will present the evaluation of the mechanical, physical and chemical properties of two-component solvent-borne polyceramic coatings with a range of formulations on metal surfaces according to analysis and tests.

Tab.1 - Surface energies of the substrates.

Substrates	Surface Energy (mJ.m-2)
Aluminium	800-950
Stainless Steel	650-1200
Polypropylene	20-40
Glass	250-500

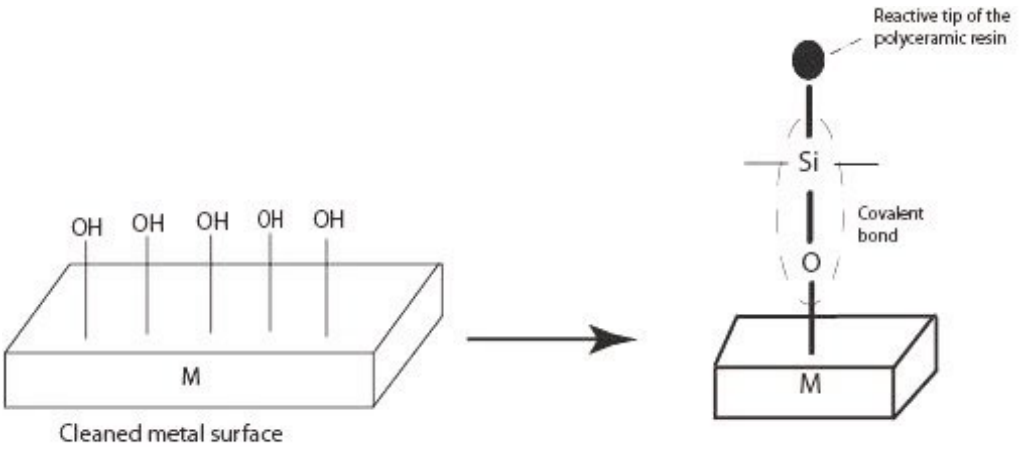

Fig.1 - Covalent bonding with metal surface and the ceramic backbone of the polyceramic resin [26-29].

MATERIALS and METHODS

The polyceramic resin is the main raw material of the coating formulation, and gives the functional properties such as hydrophobicity, ease of cleaning and oleophobicity to the coating thanks to its ceramic backbone (SiO_2) and crosslinkable polymer tips. While the ceramic in the backbone provides resistance to high temperatures and abrasion, the presence of reactive tips connected to the backbone allows the functional properties of the coating to be modified. An Acrylic resin is a thermoplastic or thermosetting plastic material based on acrylic acid, methacrylic acid or other related compounds, which is also used to obtain crosslinked polymers by treatment with polyisocyanates [18,35,36]. Furthermore, one of the main reasons for use the acrylic resin in the formulation is that it increases the slipperiness of the surface, similar to the effect of silicone additives, which increases the scratch resistance [23]. The solvents were selected from the benzene, ester or ketone groups. Esters are organic compounds wherein the hydrogen atom of a hydroxyl group is replaced by an organic group [37]. Benzene, a member of the class of organic compounds called arene or aromatic hydrocarbons, has the molecular formula C6H6 [38]. Ketones are organic compounds which having a carbonyl functional group, i.e. a carbon-oxygen bond. Their chemical structure is RC (= O) R '. The carbon atom of this group has two remaining bonds, indicated by R and R ', that can be occupied by alkyl or aryl substituents without hydrogen substituents. These organic compounds do not have reactive groups directly linked to the carbon atom in the carbonyl group, such as -OH and -Cl [39]. Carbon Black powder of particle size 25 ± 2 nm (Anhui Herrman Impex CO., LTD) is a pigment that gives the black colour to the coating, and has a high surface area / volume ratio [40]. TiO_2 powder with 0.42 μm median particle size (DuPont de Nemours, Inc.) was used to protect the coating against ultraviolet rays, provide resistance climatic conditions and heat and give durability to the coating [41]. Isocyanate is a functional group with the formula R–N=C=O. It is used as a cross-linker based on the percentage of OH in the acrylic resin and polyceramic resin (NCO/OH ratio) [18,36]. In this study, four different kinds of blocked-isocyanates [19][15] were used, as can be seen from Fig. 2, where the process of blocking/de-blocking of NCO group is presented schematically [20].

Fig.2 - Simplified scheme of blocking/de-blocking of NCO group. B-H=blocking.

The preparation of the two-component solvent-borne polyceramic coating was as follows: Firstly, a pigment paste that includes carbon black pigment was prepared to use in the coating formulation. In order to obtain a homogeneous coating, firstly the carbon black pigment must be milled properly. The percentages of the raw materials used in the paste formulation were as follows: carbon black pigment (20-35%), acrylic resin (20-30%), solvents containing benzene, ester or ketone groups (30-50%), dispersion agent (1-2%). The pigment paste formulation was stirred at

500 rpm for 3 hours with the help of a 0.5 mm diameter zircon ball and a mixing blade with an inclined blade. In order to include the white colour in the coating, the TiO_2-containing paste was prepared as follows: TiO_2 pigment (20-35%), acrylic resin (20-30%), solvents containing benzene, ester or ketone groups (30-50%), dispersion agent (1-2%) by mixing with a 0.5 mm diameter zircon ball at 500 rpm with the help of an inclined blade mixing blade for 1 hour. After milling, the main coating formulation was prepared. The main formulation was as follows: Polyceramic resin (8 - 60%), Acrylic resin (1 - 14%), Black Paste (1 - 8%), White Paste (0.5 - 2%), solvents containing benzene, ester or ketone groups (% 30-70), Dispersing agent (0.2-1.2%). The main formulation was stirred in a zircon ball mixer at 500 rpm for 20 minutes with the help of an inclined blade mixing blade. After mixing, the crosslinker was added to the first component with a ratio determined according to the OH content in the polyceramic resin and acrylic resin (NCO/OH ratio). 1.K / 2.K, which is the ratio of component 1 containing polyceramic resin to component 2 (the cross-linker ratio) was determined, and the crosslinker was added followed by stirring for 2 minutes. Surface preparation of substrates was performed because ensuring proper surface cleaning is important for physical coatings to allow the coating to adhere to the surface. For the metal surfaces, the surface treatment was carried out in the form of sandblasting for Aluminium 1050 plate and degreasing for both SAE 304 stainless steel sheet and Aluminium 1050 plate. Degreasing was carried out with 100% pure Acetone (Prasol Chemicals Limited). After surface preparation, filtration was performed at 120 Mesh to obtain a homogeneous coating mixture [42]. Then the two-component mixture was applied to the surface with a spray gun with a nozzle diameter of 1 mm at a pressure of 4 bar.

Following the spray application, curing processes were carried out as shown in Table 2. While this work only studied the properties of polyceramic coatings on metal surfaces, additionally outside the scope of this study, film formation was obtained on plastic and glass surfaces according to the curing conditions given in Table 2.

The samples, which were analysed and tested after the curing process, are given in Table 3.

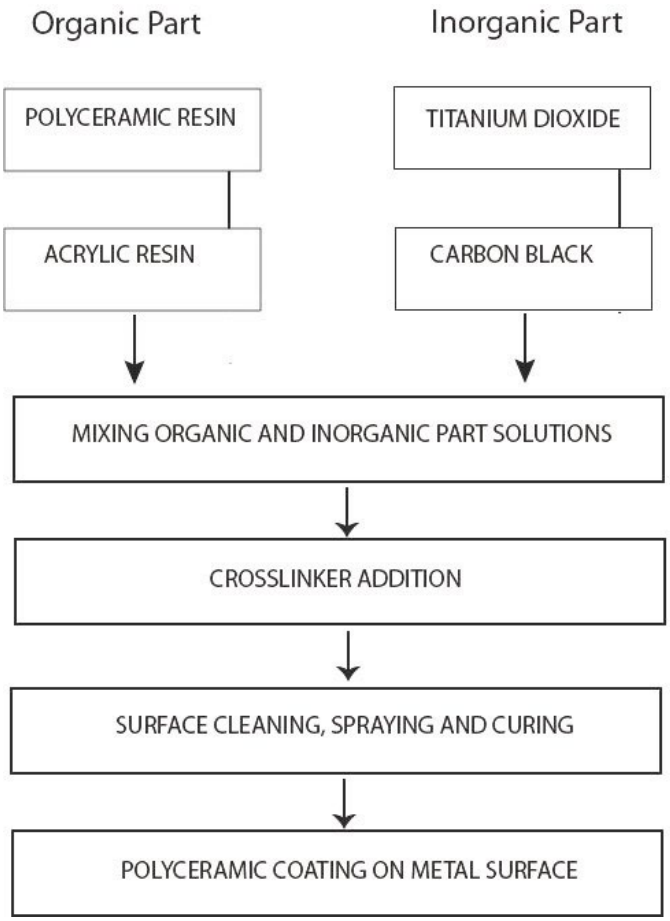

Fig.3 - Preparation scheme for Polyceramic coating.

Tab.2 - Curing processes on different substrates.

Substrates	Time (min.)	Temperature (°C)
Sandblasted Aluminium 1050 Plate SAE 304 Sheet Stainless Steel	60-120	120-180
Polypropylene Sheet	120-150	50-80
SA-66 Glass Plate	60-120	450-650

Tab.3 - Sample contents according to component 1 and component 2.

Samples	Component 1	Component 2
PLC-13	Polyceramic resin (8 - 54%) Acrylic resin (1 - 14%) Black Paste (1 - 8%) White Paste (0.5 - 2%) Solvents containing benzene, ester or ketone groups (% 30-50) Dispersing agent (0.2-1.2%) Fluorine solvent (%15-42)	Isocyanate 3
PLC-19 PLC-19.1 PLC-19.2 PLC-19.3	Polyceramic resin (8 - 60%) Acrylic resin (1 - 14%) Black Paste (1 - 8%) White Paste (0.5 - 2%) Solvents containing benzene, ester or ketone groups (% 30-70) Dispersing agent (0.2-1.2%)	Isocyanate 1 Isocyanate 2 Isocyanate 3 Isocyanate 4
PLC-21	Polyceramic resin (15 - 65%) Acrylic resin (2 - 14%) Black Paste (1 - 8%) White Paste (0.5 - 2%) Solvents containing benzene, ester or ketone groups (% 30-60) Dispersing agent (0.2-1.2%)	Isocyanate 3

EXPERIMENTAL

The contact angle between the coating and the metal substrate was measured by a goniometer (Terralab Laboratuvar Malzemeleri San. ve Tic. A.Ş, Attention Theta), which automatically analyses the time-dependent drop shape by recording drop images. A particular solid, liquid and vapor system at a given temperature and pressure has a unique equilibrium contact angle, and the wettability of a solid surface is given by the Young equation. The equilibrium contact angle indicates the relative strength of the interaction between liquid, solid and vapor molecules [43]. A comparison of contact angle results for different formulations is given in Figure 3.1. FTIR analysis was performed with a Perkin Elmer Spectrum Two FT-IR Spectrometer and was used to determine the chemical bonds in the coatings before the single-component trials and after crosslinking in the 2-component trials. Fourier transform infrared spectroscopy (FTIR) is a technique used to obtain the infrared absorption spectrum of a solid, liquid or gas, as well as collecting high spectral resolution data over a wide spectral range. This provides a significant advantage over a dispersive spectrometer, which measures the density in a narrow wavelength range at a given time [44]. The results of the analysis are given in Figure 3.2. and Figure 3.3. Thermogravimetric analysis (Perkin Elmer, TGA 4000) of single- and two-component coating samples was

carried out according to the TS ISO EN 11358-1 standard. Thermogravimetric analysis or thermal gravimetric analysis (TGA) is a method of thermal analysis in which the mass of a sample placed in the instrument is measured over time as a function of temperature. This measurement provides information about physical events such as phase transitions, absorption, adsorption and desorption; as well as chemical events involving chemical reactions, thermal decomposition, and solid-gas reactions (e.g., oxidation or reduction) [45]. In addition to the decomposition temperatures of our samples determined by TGA analysis, temperature-related mass losses are given in Figure 3.4. Scanning Electron Microscopy / Energy Dispersive Spectrometer (SEM / EDS) Analysis was performed for the final product PLC-21. In scanning electron microscopy (SEM), a highly energetic and focused electron beam scans the sample and provides information on the chemical composition of the sample using an energy-dispersing spectrometer (EDS) detector, as well as a high-magnification view of the sample's morphology [46]. SEM-EDS is mainly used in the characterization of inorganic materials, but recently its application has been expanded to examine organic-based samples such as polymers. The SEM / EDS analysis given in Image 3.1 and Fig. 3.5., gives us information about the microstructure and chemical content of the final product PLC-21. Tests conducted according to the ASTM Standards were as follows: the Mandrel Bend Test (ASTM D522) was carried out to evaluate the ability of the coating to withstand cracking when elongated. With this test it is possible to measure the flexibility of a coating on flexible substrates [47]. The Measuring Adhesion by Tape (ASTM D3359) test was carried out to assess the adhesion level of the coatings applied to metal surfaces [48]. The Film Hardness by Pencil Test (ASTM D3363) was performed to measure the hardness of the organic coating film and to compare it with polymeric and ceramic coatings according to their hardness values varying from H to 9H, according to ASTM [49]. In addition, the corrosion test determines the corrosion resistance of materials under certain environmental conditions including temperature, humidity and salinity [50]. Therefore, the corrosion test on the coatings was carried out at via the salt fog test at 35 ° C with 5% saline solution under laboratory conditions according to ASTM B117 [51].

RESULTS AND DISCUSSION

The wettability of organic surfaces is determined by the nature and packing of atoms or groups of atoms on the surface of a solid and is otherwise independent of the nature and arrangements of the underlying atoms or molecules [52]. Surfaces are classified as hydrophobic if there is a non-polar interaction with water, or hydrophilic if there is a polar interaction with water [53]. Polarity plays an important role in wettability, because the interfacial tension is largely determined by the polarity and can affect the adhesion of the coating [54]. In order to study the wettability and hydrophilic/hydrophobic behaviour of the obtained coatings, contact angle tests were carried out on coated metal substrates. The contact angle analysis showed that the wetting angles of PLC-21 were about 90 °; another striking result is that PLC-13 had a contact angle of up to 115 ° (Figure 2.3.1). A coating is defined as hydrophobic when 0 > 90, and a coating with a larger contact angle usually features stronger hydrophobicity [55]. This is because the high contact angle is caused by a high fluorine content in the formulation, which has a surface tension reducing effect in PLC-13 [56]. Although we achieved a high contact angle in PLC-13, it did not meet expectations in terms of mechanical properties. In addition, this analysis found evidence for the effects of different types of isocyanate on coatings constituted with same first component. It is notable that among the samples with the same first component, with ~100° contact angle value, isocyanate-2 made the highest contribution to the hydrophobicity of the coating, and with ~75° contact angle value, isocyanate-4 made the lowest contribution to the hydrophobicity of the coating. Our results demonstrated that the contact angle of ~90° shown by PLC-21 was provided by addition of TiO_2 to the polyceramic resin containing a SiO_2 backbone [24]. This physical property of PLC-21 ensures water retention and easy cleaning on metal surfaces where the coating is used [57]. Due to the accumulation of dust, dirt or air pollution from day-to-day use, surfaces become unable to maintain their original performance, and the renewal of the surfaces causes loss of money, labour and energy [58]. Thanks to their easy-to-clean feature, Polyceramic coatings can stand out in applications such as the body, motor or exhaust pipes of motorcycles or cars or even metal eyeglass frames.

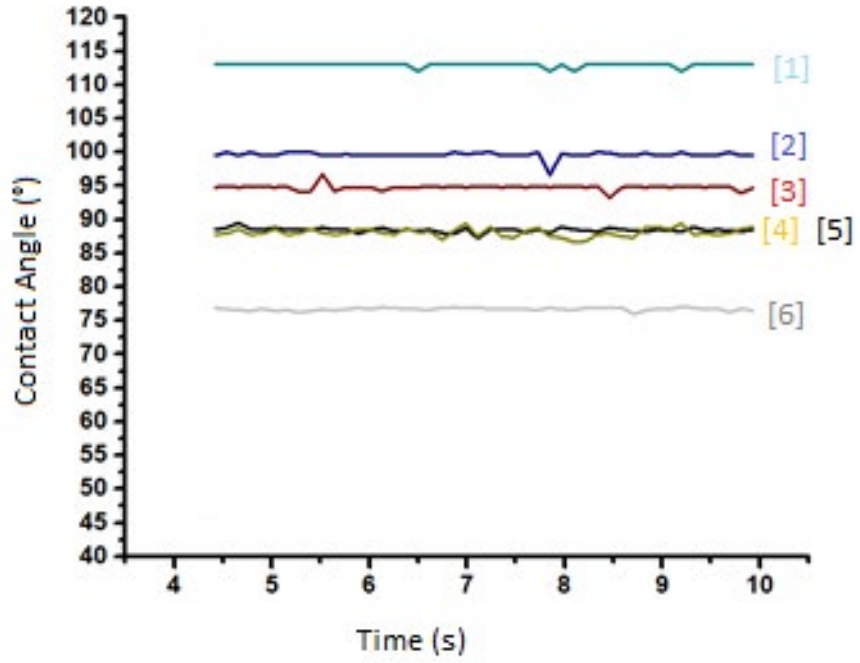

Fig.3/1 - Contact angle analysis results ; [1]: PLC-13, [2]: PLC-19.1 , [3]: PLC-19 , [4]: PLC-19.2 , [5]: PLC-21 , [6]: PLC-19.3

In this study, FT-IR analysis of the cross-linked states of PLC-19.2 and PLC-21 samples were performed as seen in Figure 3.2. These analyses provided information on chemical bonds in the final products resulting from crosslinking. In the FTIR spectra of the polyceramic coatings, the bands at ~ 3385 cm^{-1} correspond to the N–H stretching mode [59]. Anhydrous ammonia is a solvent which shows evidence of extensive hydrogen bonding. Despite its water-like behaviour, it has less hydrogen bonding, which is responsible for the low freezing and boiling points of anhydrous ammonia compared to water or alcohols. While water molecules exhibit hydrogen bonding in two directions, ammonia is thought to form linear species with only one hydrogen atom per molecule taking part in a hydrogen bond. The FTIR spectrum of liquid ammonia exhibits a complex envelope between 3100 and 3500 cm^{-1} composed primarily of N-H stretching bands. Furthermore, according to the literature [59,60], it was found that ClO4- ion breaks the hydrogen bonds in the solvent, and as a result the stretching mode frequency is increased in the presence of ClO_4-. Cl- ions, which were found to be present in the coating by EDS analysis as seen in Figure 3.6., may have had an effect on this stretching mode. The 3385 cm-1 band is assigned to the antisymmetric stretching mode of N-H bonds [59,60]. Another observed peak in the infrared Fourier transform spectrum analysis at ~ 2950 cm^{-1} is assigned to the C–H symmetric stretching mode [61-64]. Another bond seen by the analysis is the bond of silicon, which is found in the polyceramic resin, with hydrogen. The Si-H stretching band, which generally occurs in the range of 2000 to 2100 cm^{-1}, was observed around 2125 cm-1 [65]. This small shift may be due to the proximity fluoride, with a high electronegative value, to Si-H bonds [65-67]. The peak located at around 1250 cm-1 can be correlated with the Si–CH_3 symmetric bending mode. The Si—CH_3 group can easily identified as a strong, sharp band at about 1260 cm-1 in conjunction with one or more strong bands in the 865-750 cm^{-1} range. In this case, while methyl groups bonded to silicon atoms undergo the same C-H stretching and bending vibrations as a CH_3 bonded to a carbon atom, the Si-CH_3 group shows different band positions from C-CH_3 due to electronic effects. The absorption attributed to the symmetric bend vibration of the Si–CH_3 group produces a very intense band at 1260 ± 5 cm^{-1}. The chemical bonds observed in the two-component samples enabled us to determine the relationships between the materials used in the formulation of the polyceramic coatings [68-70].

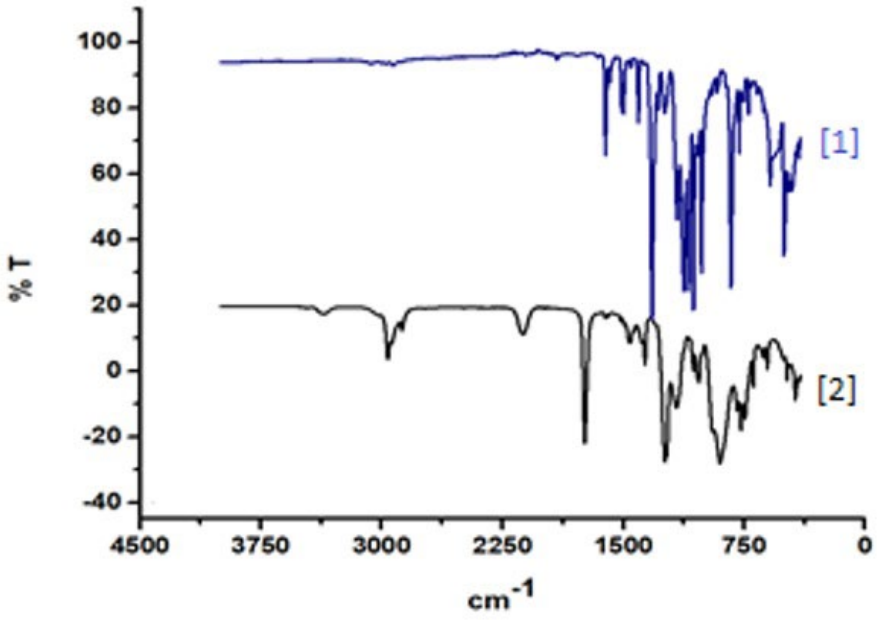

Fig.3/2 - FTIR Analysis; [1]: PLC- 21 , [2]: PLC- 19.2

Thermogravimetric analysis was used to examine the thermal behaviour of the polyceramic coatings. Fig. 3.4 shows the mass loss occurring in the coating as a function of temperature. In the first thermal event in the TGA curves for the Polyceramic coatings, there is a significant weight drop of ~30% between about 100 and 200 °C, due to the loss of organic solvents [71,72]. The second thermal event is the mass loss between 200 and 400 °C. This mass loss is associated with the decomposition of the acrylic resin and the reactive tips of the polyceramic resin in the formulation [73]. A third thermal event is mass loss of the formulations of between 65 and 80% at temperatures up to 850 °C. Consequently, PLC-19.2 and PLC-21 have non-degraded solid percent between 20 and 25 at 850 °C. Thus, these samples could resist temperatures up to 850 °C without complete degradation due to the TiO_2 additive and the SiO_2 backbone found in the polyceramic resin.

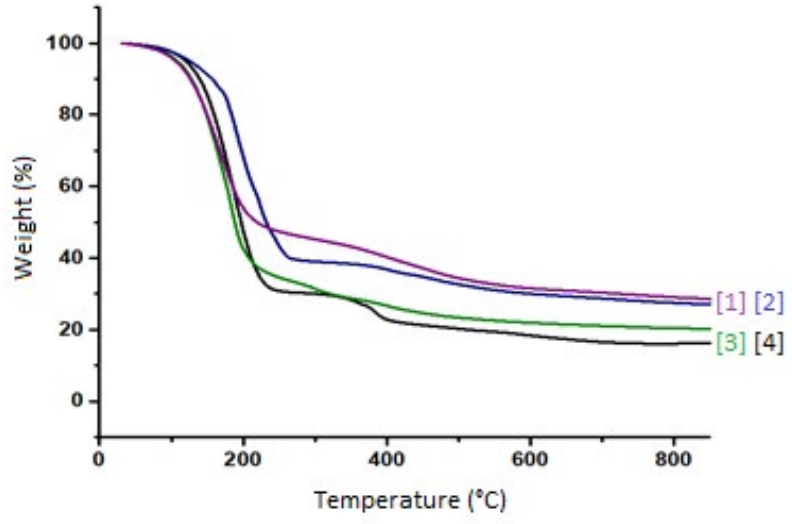

Fig.3/4 - One TGA analysis comparisons. [1]: PLC- 13, [2]: PLC- 19.1, [3]: PLC- 21, [4]: PLC- 19.2

In order to determine the distribution of the constituent elements, chemical microanalysis and crystal structures on the surface of the final polyceramic coating sample, PLC- 21, SEM-EDS analysis was conducted. The crystal structures of particles are shown in Figure 3.5. The results of the surface chemical characterisation of each of the particles are given in Figure 3.6. All particles contain Si, O, Cl and Na, which are mostly provided from the Polyceramic resin and acrylic resin. Most particles also contain detectable levels of K and Ca. Occasional instances of F and C were also identified. When the SEM images are examined, the first thing that draws attention is the formation of hybrid particles derived from different nucleation mechanisms. As can be seen in Figure 3.5a, dendritic crystals formed in the coating. The average diameter of these dendritic crystallites was 6.35 µm and Cl, Si, Na, K, O were detected in the specified region according to EDS analysis as seen in Fig. 3.5a. When the 2nd selected region shown in Figure 3.5b was examined, a polygonal crystal with an average diameter of 5.71 µm was observed. However, according to EDS analysis, Cl, Si, Na, O, and K were detected in the structure and it was noted that the structure contained these elements in the same concentrations as in the dendritic crystals, as seen in Figure 3.6a and Figure 3.6b. According to EDS analysis, chloride (Cl-) and SiO_2 is expected in these two types of crystals. Cl and Si in the crystals indicate the presence of the Silicon backbone and the reactive Cl ends in the polyceramic resin. When the SEM image of the third indicated area is examined, a polygon crystal can be seen with average diameter of 15 µm. According to the results of EDS analysis, unlike the other two regions, the presence of Calcium (Ca) and Titanium (Ti) is remarkable in this region. Another remarkable finding according to the EDS result is the dominance of Silicon (Si) concentration in this region. When the fourth identified particle was examined, it was found to be a polygonal crystal with a diameter of 19.2 µm (see Figure 3.5d). As shown in Figure 3.6d, Carbon (C) from the use of Carbon black and Fluorine (F) from the polyceramic resin reactive ends were detected in this particle.

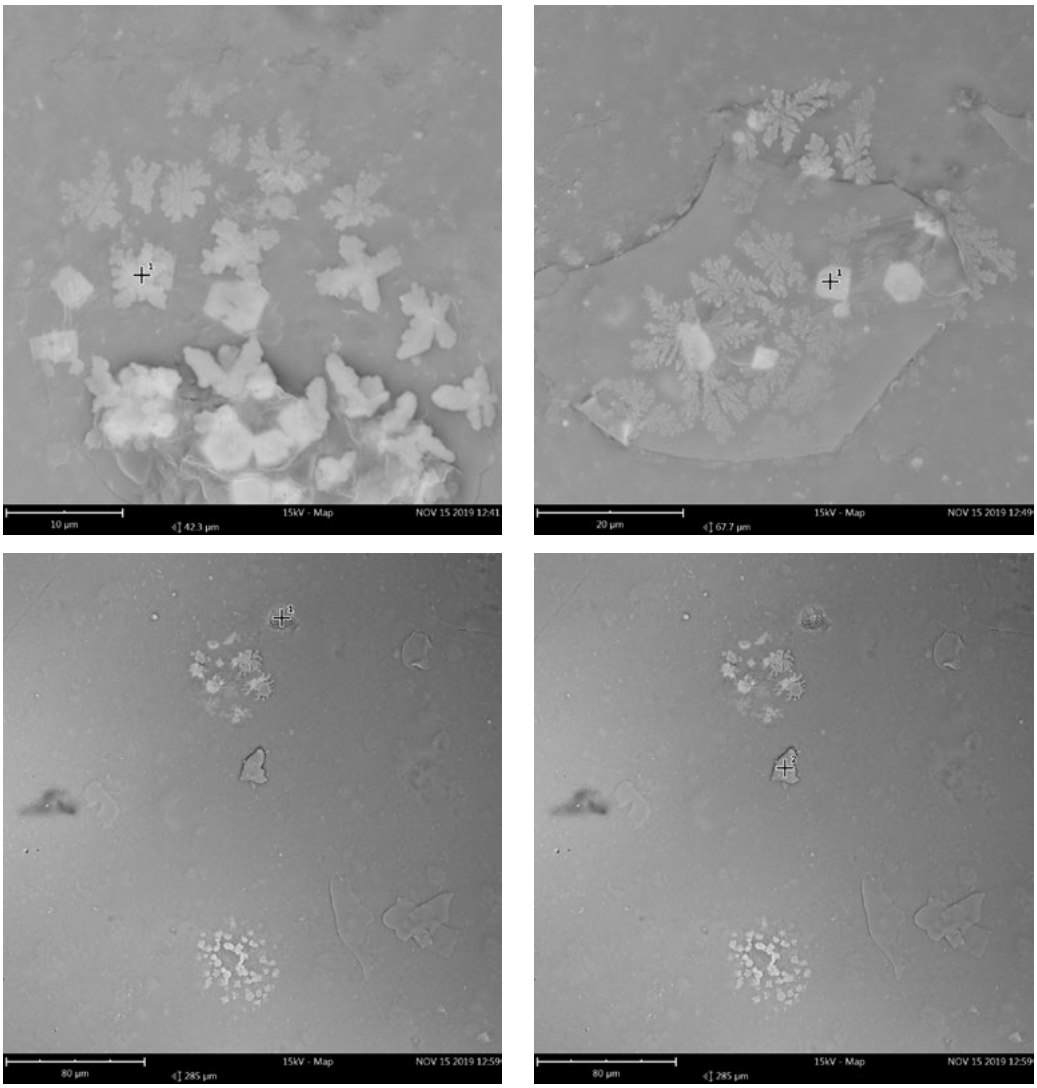

Fig.3/5 - SEM images of the PLC- 21 sample with different regions (a ,b, c and d) of the sample surface.

a)

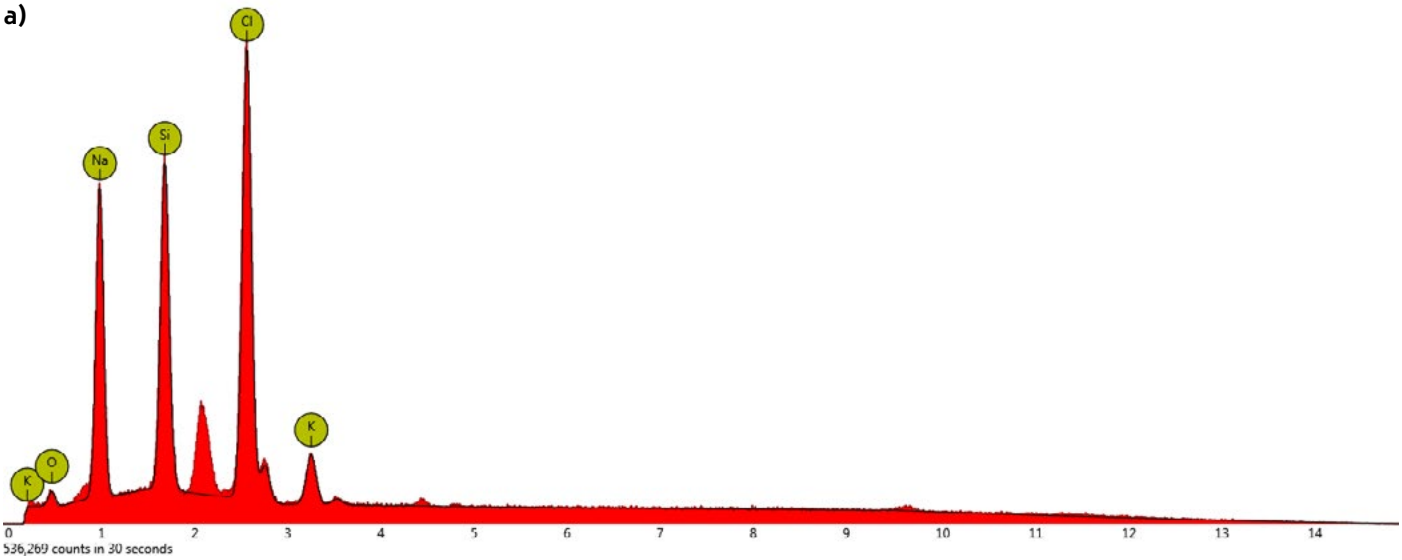

Atomic Number	Element Symbol	Element Name	Confidence	Concentration	Error
17	Cl	Chlorine	100.0	35.9	0.4
14	Si	Silicon	100.0	18.4	0.5
11	Na	Sodium	100.0	33.7	0.6
19	K	Potassium	100.0	5.6	1.4
8	O	Oxygen	100.0	6.4	3.9

b)

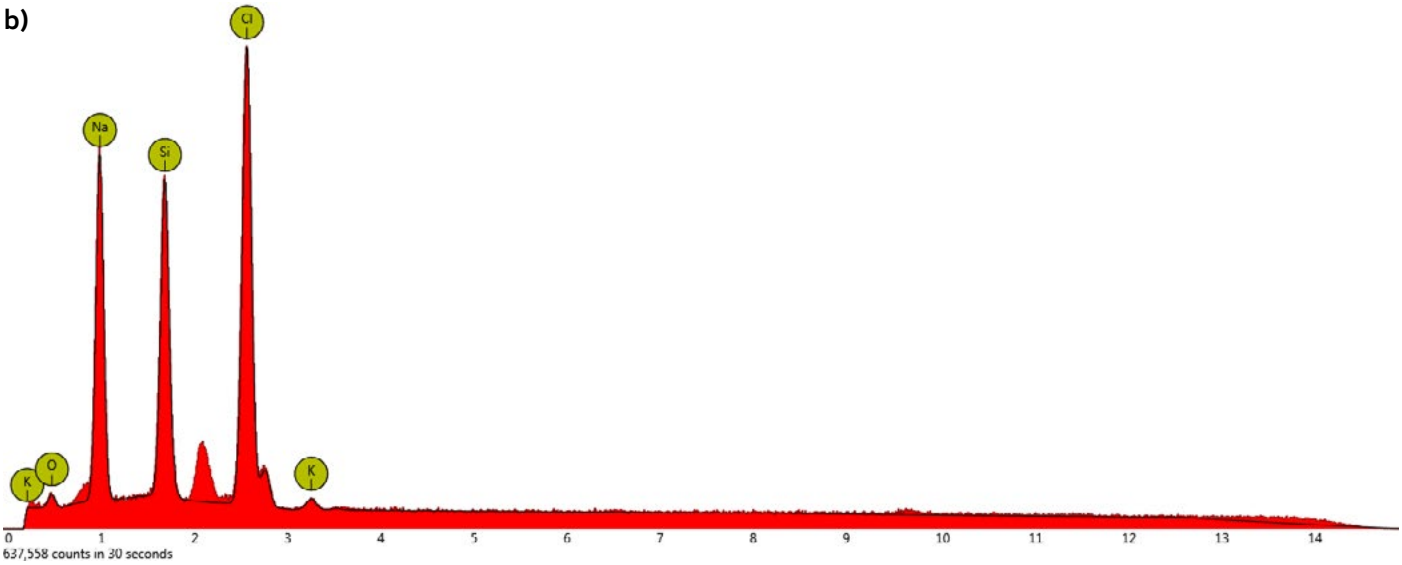

Atomic Number	Element Symbol	Element Name	Confidence	Concentration	Error
17	Cl	Chlorine	100.0	37.7	0.4
14	Si	Silicon	100.0	18.5	0.5
11	Na	Sodium	100.0	36.9	0.5
19	K	Potassium	100.0	1.3	4.2
8	O	Oxygen	100.0	5.7	4.3

c)

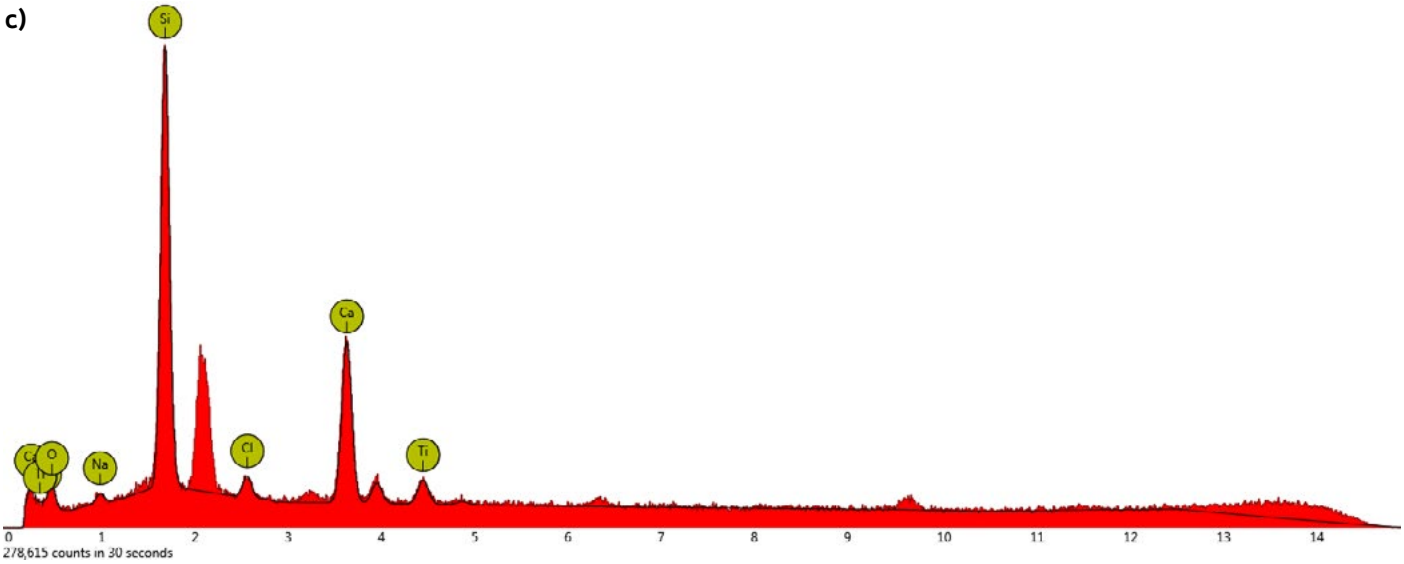

Atomic Number	Element Symbol	Element Name	Confidence	Concentration	Error
14	Si	Silicon	100.0	36.9	0.7
20	Ca	Calcium	100.0	28.1	1.1
22	Ti	Titanium	50.0	6.7	3.6
17	Cl	Chlorine	100.0	3.2	4.6
8	O	Oxygen	100.0	22.7	3.9
11	Na	Sodium	Manual	2.5	9.3

d)

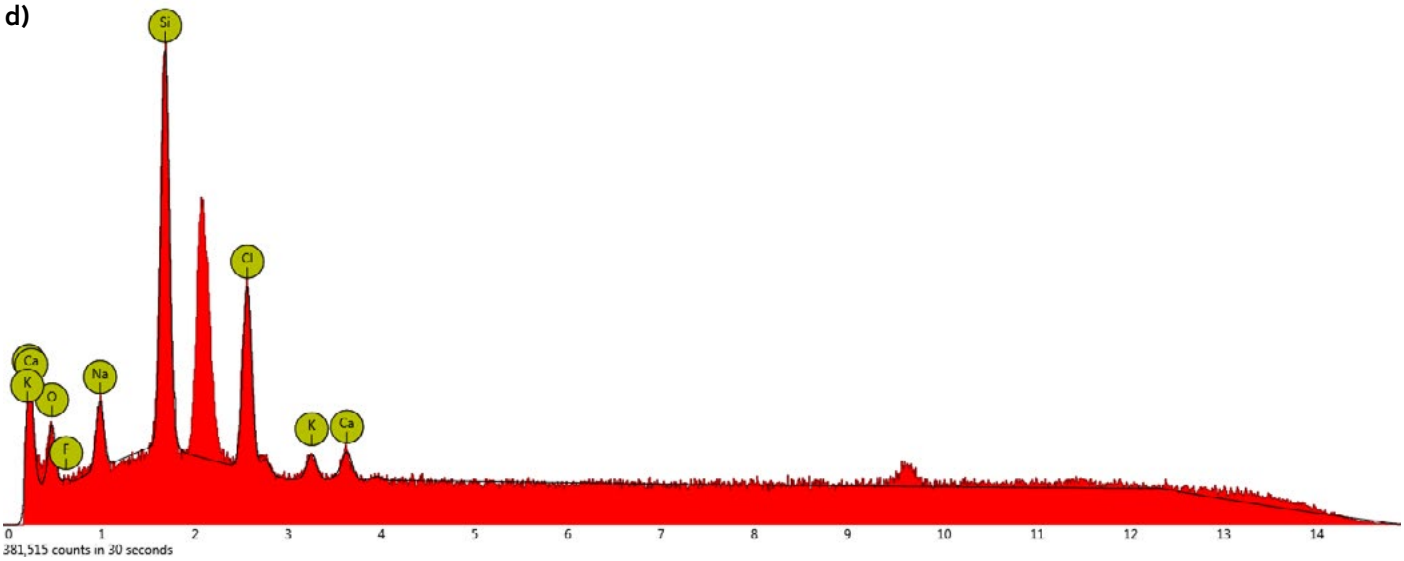

Atomic Number	Element Symbol	Element Name	Confidence	Concentration	Error
14	Si	Silicon	100.0	23.7	0.8
17	Cl	Chlorine	100.0	17.8	1.3
6	C	Carbon	100.0	10.6	1.9
11	Na	Sodium	100.0	11.0	2.8
8	O	Oxygen	100.0	27.5	2.8
20	Ca	Calcium	100.0	3.6	4.6
19	K	Potassium	100.0	3.2	4.9
9	F	Fluorine	100.0	2.6	20.7

Fig.3/6 - a, b, c and d show the graphical representation and concentration values of the elements according to the EDS results for different regions of the PLC-21 surface, respectively.

The Mandrel Bend Test (ASTM D522) was performed on the coated SAE 304 stainless steel sheet as it can only be applied to flexible substrates. The coated sample was held in between the mandrel and drawbar. The lever was then moved to 180° at a constant velocity, held for one second, and the coated samples were visually examined for cracks along the bent surface. As a result of 180° degree bending, only PLC-21 was able to withstand 180° bending without cracking. Accordingly, we can infer that the increased proportion of polyceramic resin adds more flexibility to the coating.

The Measuring Adhesion by Tape (ASTM D3359) test was carried out [74] to evaluate the coating adhesion to a metal substrate. PLC-21 was applied to steel sheet and a crosshatch cut was made, with 6 cuts 2 mm apart. Pressure-sensitive tape was applied over the crosshatch cut and then the tape was smoothed into place over the area of the incisions. The tape was then removed by pulling it off rapidly back over itself as close to an angle of 180° as possible, and the adhesion of the coating to the steel was assessed on a 0B to 5B scale as shown in Figure 4 [48]. According to the test result, a 5B adhesion rating was obtained for the coating.

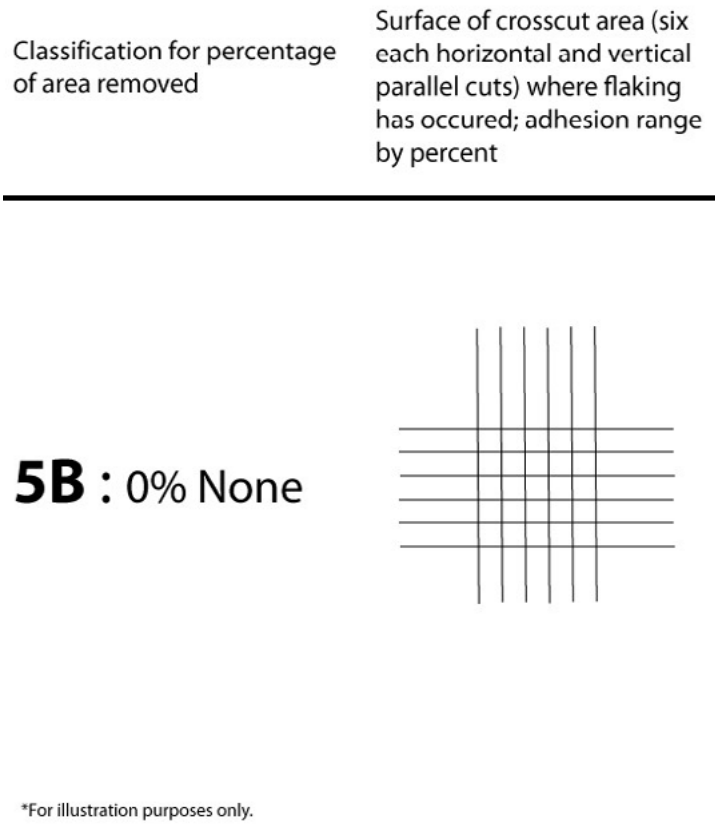

Fig.4 - Illustration of adhesion test result.

The Film Hardness by Pencil Test (ASTM D3363) was performed on the SAE 304 stainless steel sheet with an Elcometer 501 Pencil Hardness Tester to determine the hardness of the coating materials. In order to carry out this test, graphite pencils of different hardness were moved in a certain direction. Scratches of at least 6.5 mm were made going from the hardest to lowest pencil grade. The pencil tip was polished before each test in order to provide a smooth chip-free surface [75]. Coating hardness relative to the graphite pencils is determined by the softest pencil that will leave a scratch on the surface of the coating [49]. According to the test, an 8H pencil hardness value was obtained for the coating.

The main function of corrosion-resistant coatings is to create a barrier between the surface metal and a corrosive environment. A corrosion-resistance test is used to measure the ability of a protective coating to act as a barrier between the metal substrate and the environment. The damaged coatings are evaluated by physical appearance (surface morphology, pitting and chemical deposited products, and pits) [76]. In this study, the salt fog test (ASTM B117) was carried out for PLC-21 using 5% saline solution at 35 ° C in a drying oven. The test showed that there was no blister formation or flaking of the coating on the PLC-21 surface, even for time periods longer than 700 h. This result was an indication of the interaction between hydroxyl groups on the metal surface and the polyceramic coating, which increases the adhesion of the coating with the metal surface and prevents the diffusion of Cl- ions into the coating to increase the ionic resistance.

CONCLUSIONS

Collectively, our results demonstrate that it is possible to increase the service life of metal surfaces by developing a coating that can show the superior properties of polymer and ceramic coatings together. In this study, the polyceramic coating, which was characterised by TGA, FTIR, and SEM / EDS analysis, was applied to two metal substrates, sandblasted plate Al1050 and SAE 304 stainless steel sheet, by spraying at a pressure of 5 bar with a 1 mm nozzle diameter spray gun. After curing at temperatures ranging from 120 and 180 ° C for times ranging from 60 to 120 minutes, coatings that are extremely hard (8H), perfectly adhered to the metal substrate (level 5B), hydrophilic (~ 90 °contact angle), and highly flexible (180° mandrel bending) were achieved, which showed high corrosion resistance in a salt fog test conducted at 35 °C with 5% salt solution for 700 hours. Furthermore, besides metal surfaces, film formation was achieved on polymer and glass surfaces under suitable curing conditions due to its low surface energy. In line with this result, it is believed that the physical, chemical and mechanical properties of polyceramic coatings on different substrates can be improved in future studies. The main conclusion that can be drawn is that the aforementioned properties allow the polyceramic coatings to be used in high temperature applications that are not suitable for polymeric coatings, at temperatures up to 650 ° C on metal surfaces with complex geometries, and provide a long service life due to their corrosion resistance.

REFERENCES

[1] A. Yamano and H. Kozuka, "Perhydropolysilazane-derived silica-polymethylmethacrylate hybrid thin films highly doped with spiropyran: Effects of polymethylmethacrylate on the hardness, chemical durability and photochromic properties," Thin Solid Films, 2011.

[2] M. H. Uğur, E. Çakmakçı, A. Güngör, and N. Kayaman-Apohan, "Surface properties of sol–gel-based fluorine-containing ceramic coatings," J. Sol-Gel Sci. Technol., 2018.

[3] D. H. Kim, H. M. Lim, S. M. Kim, B. M. Kim, D. S. Kim, and S. H. Lee, "Effect of colloidal silica contents in the organic-inorganic hybrid coatings on the physical properties of the film on the metal surface," in Solid State Phenomena, 2007.

[4] L. Zhang et al., "Key issues of MoSi2-UHTC ceramics for ultra high temperature heating element applications: Mechanical, electrical, oxidation and thermal shock behaviors," J. Alloys Compd., 2019.

[5] J. C. Han, "Thermal shock resistance of ceramic coatings," Acta Mater., 2007.

[6] M. F. H. Wolff, V. Salikov, S. Antonyuk, S. Heinrich, and G. A. Schneider, "Novel, highly-filled ceramic-polymer composites synthesized by a spouted bed spray granulation process," Compos. Sci. Technol., 2014.

[7] R. Bermejo and R. Danzer, "Mechanical Characterization of Ceramics: Designing with Brittle Materials," in Comprehensive Hard Materials, 2014.

[8] J. J. Licari, "Chemistry and Properties of Polymer Coatings", in Coating Materials for Electronic Applications: Polymers, Processing, Reliability, Testing. 2003.

[9] L. McKeen, "Polytetrafluoroethylene (PTFE)", in Fluorinated Coatings and Finishes Handbook, William Andrew Publishing, 2006.

[10] Walter Hellerich, Günther Harsch, Erwin Baur, Werkstoff-Führer Kunststoffe: Eigenschaften, Prüfungen, Kennwert, 10th ed., 2010.

[11] C. Mateus, S. Costil, R. Bolot, and C. Coddet, "Ceramic/fluoropolymer composite coatings by thermal spraying - A modification of surface properties," Surf. Coatings Technol., 2005.

[12] A. S. Wagh, Chemically Bonded Phosphate Ceramics: Twenty-First Century Materials with Diverse Applications: Second Edition. 2016.

[13] Jesse Burl Thompson , Hilda Cantor Tadio , Salvador A. Tostado , Apolinar Alvarez JR. , Polyceramic-coated Tool For Applying A Flowable Composition , Southavenue Westfield, Nj 07090 (Us) , 2005.

[14] T. L. Metroke, R. L. Parkhill, and E. T. Knobbe, "Passivation of metal alloys using sol-gel-derived materials - A review," Prog. Org. Coatings, 41 233–238 , 2001.

[15] M. L. Zheludkevich, R. Serra, M. F. Montemor, and M. G. S. Ferreira, "Oxide nanoparticle reservoirs for storage and prolonged release of the corrosion inhibitors," Electrochem. commun., 7 836–840 , 2005.

[16] M. L. Zheludkevich, R. Serra, M. F. Montemor, I. M. Miranda Salvado, and M. G. S. Ferreira, "Corrosion protective properties of nanostructured sol-gel hybrid coatings to AA2024-T3," Surf. Coatings Technol. 200(9):3084-3094, 2006.

[17] Y. Wang and X. Gong, "Special oleophobic and hydrophilic surfaces: approaches, mechanisms, and applications," Journal of Materials Chemistry A. 2017.

[18] E. A. Papaj, D. J. Mills, and S. S. Jamali, "Effect of hardener variation on protective properties of polyurethane coating," Prog. Org. Coatings, 2014.

[19] M. S. Rolph, A. L. J. Markowska, C. N. Warriner, and R. K. O'Reilly, "Blocked isocyanates: From analytical and experimental considerations to non-polyurethane applications," Polymer Chemistry. 2016.

[20] J. Kozakiewicz, J. Przybylski, K. Sylwestrzak, and I. Ofat, "New family of functionalized crosslinkers for heat-curable polyurethane systems-a preliminary study," in Progress in Organic Coatings, 2011.

[21] M.S. Um, D.S. Ham, S.K. Cho, S.-J. Lee, K.J. Kim, J.H. Lee, S.-H. Choa, H.W. Jung, W.J. Choi, Prog. Org. Coat., 97, 2016, pp. 166–174

[22] I. Skeist and J. Miron, "Introduction to Adhesives," in Handbook of Adhesives, 1990.

[23] A. Bubat and W. Scholz, "Silicone additives for paints and coatings," Chimia (Aarau)., 2002.

[24] J.-J. Wang, D.-S. Wang, J. Wang, W.-L. Zhao, C.-W. Wang, Surf. Coat. Technol. 205, 2011, pp. 3596–3599.[25] G. L. Jialanella, "Advances in bonding plastics," in Advances in Structural Adhesive Bonding, 2010, pp. 246-250.

[26] Ricky Bennett, Eric Hanson, "Low Surface Energy Coatings, Rewrites the Area Ratio Rules", in IPC APEX EXPO Conference & Exhibition, San Diego, California, USA, 2013.

[27] B. Arkles, "Tailoring surfaces with silanes," Chemtech, 1977, 7(12):766-778.

[28] D. Amouzou, L. Fourdrinier, F. Maseri, and R. Sporken, "Formation of Me-O-Si covalent bonds at the interface between polysilazane and stainless steel," Appl. Surf. Sci., 2014.

[29] Richard M. Laine, Christopher L. Soles, David J. Krug, Hyun Wook Ro, Rockville, Vera Nikolova Popova-Gueorguieva, Silsesquioxane Derived Hard, Hydrophobic And Thermally Stable Thin Films And Coatings For Tailorable Protective And Multi-Structured Surfaces And Interfaces, US20110062619A1, March 17, 2011.

[30] K. S. Aneja, S. Bohm, A. S. Khanna, and H. L. M. Bohm, "Graphene based anticorrosive coatings for Cr(VI) replacement," Nanoscale, 2015.

[31] J. Glazer, "Monolayer studies of some ethoxylin resin adhesives and related compounds," J. Polym. Sci., 1954.

[32] M. NAKAZAWA, "Mechanism of Adhesion of Organic Compounds to Metal Surfaces," J. Japan Soc. Colour Mater., 1995.

[33] G. H. Koch, M. P. H. Brongers, N. G. Thompson, Y. P. Virmani, and J. H. Payer, "CORROSION COSTS AND PREVENTIVE STRATEGIES Publication No . FHWA-RD-01-156," Corrosion, 2001.

[34] Edward McCafferty, Introduction to Corrosion Science 2010th Edition, 2010.

[35] Stoye, D.; Funke, W.; Hoppe, L.; et al. "Paints and Coatings", Ullmann's Encyclopedia of Industrial Chemistry, Weinheim: Wiley-VCH, 2006.

[36 Hubert Baumgart, Uwe Meisenburg, Karl-Heinz Joost, "Thermally Setting Substance Mixture And Use Thereof", WO2002016461, February 28, 2002. (PATENT)

[37] A. D. McNaught and A. Wilkinson, IUPAC. Compendium of Chemical Terminology, 2nd ed. (the "Gold Book"). 1997.

[38] "New Edition of the 'IUPAC Blue Book'Nomenclature of Organic Chemistry—IUPAC Recommendations and Preferred Names 2013," Chem. Int., 2014, pp. 01-04.

[39] Serban C. Moldoveanu, "Pyrolysis of Organic Molecules with Applications to Health and Environmental Issues," 2nd ed, 2019.

[40] International Carbon Black Association, "What is carbon black", Archived from the original on 2009-04-01. Retrieved 2009-04-14.

[41] L. S. Dubrovinsky et al., "Materials science. The hardest known oxide.," Nature, 2001, 410 (6829): 653–654.

[42] S. Ebnesajjad, Expanded PTFE Applications Handbook: Technology, Manufacturing and Applications. 2017, pp. 213-231.

[43] Z. Shi, Y. Zhang, M. Liu, D. A. H. Hanaor, and Y. Gan, "Dynamic contact angle hysteresis in liquid bridges," Colloids and Surfaces A Physicochem. and Eng. Asp.555, 2018, pp. 365-371.

[44] P. R. Griffiths and J. A. De Haseth, Fourier Transform Infrared Spectrometry: Second Edition, Wiley-Blackwell, 2006.

[45] A. W. Coats and J. P. Redfern, "Thermogravimetric analysis. A review," Analyst, 88 (1053): 906–924, 1963.

[46] A. V. Girão and G. Caputo, Characterization and Analysis of Microplastics : Application of Scanning Electron Microscopy–Energy Dispersive X-Ray Spectroscopy (SEM-EDS)," Compr. Anal. Chem., 2016, ch 6.

[47] American Society for Testing and Materials. ASTM D522 / D522M-17, Standard Test Methods for Mandrel Bend Test of Attached Organic Coatings; 2017
[48] American Society for Testing and Materials. ASTM D3359-17, Standard Test Methods for Rating Adhesion by Tape Test;2017
[49] American Society for Testing and Materials. ASTM D3363-05(2011)e2, Standard Test Method for Film Hardness by Pencil Test; 2011
[50] Robert Baboian, Corrosion Tests and Standards - Application and Interpretation, 2005, pp. 7-25.
[51] ASTM B117-19, Standard Practice for Operating Salt Spray (Fog) Apparatus, ASTM International, West Conshohocken, PA, 2019, www.astm.org
[52] L. Lee, T. Dow, Adhesion of high polymers . II, J. Polym. Sci. Par A-2. 5 1103–1118, 1967.
[53] N. Giovambattista, P. G. Debenedetti, and P. J. Rossky, "Effect of surface polarity on water contact angle and interfacial hydration structure," J. Phys. Chem. B 111, 2007.
[54] M. Bragaglia, I. Cacciotti, V. Cherubini, and F. Nanni, "Influence of organic modified silica coatings on the tribological properties of elastomeric compounds," Wear, 2019.
[55] G. Li, J. Yue, C. Guo, and Y. Ji, "Influences of modified nanoparticles on hydrophobicity of concrete with organic film coating," Constr. Build. Mater., 2018.
[56] L. Mittal, Contact Angle, Wettability and Adhesion, Volume 5. 2008, pp. 279-285.
[57] V. A. Ganesh, H. K. Raut, A. S. Nair, and S. Ramakrishna, "A review on self-cleaning coatings," Journal of Materials Chemistry. 2011.
[58] S. S. Latthe et al., "Self – cleaning superhydrophobic coatings: Potential industrial applications," Prog. Org. Coatings, 2019.
[59] C. Steinbach, and U. Buck, "Infrared spectroscopy of large ammonia clusters as a function of size," J. Chem. Phys., 2006.
[60] J J Lagowski, The Chemistry of Nonaqueous Solvents. Volume IV Solution Phenomena and Aprotic Solvents, Academic Press-2. HYDROGEN BONDING PHENOMENA – 3.RAMAN SPECTROPOY, 1976.
[61] E. H. Lieb, D. C. Mattis, and F. J. Dyson, "Mathematical Physics in One Dimension: Exactly Soluble Models of Interacting Particles," Phys. Today, 1967.
[62] P. Nallasamy, P. M. Anbarasan, and S. Mohan, "Vibrational spectra and assignments of cis- and trans-1,4-polybutadiene," in Turkish Journal of Chemistry, 2002.
[63] R. Lees et al., "FTIR SYNCHROTRON SPECTROSCOPY OF THE ASYMMETRIC C-H STRETCHING BANDS OF METHYL MERCAPTAN (CH3SH) – A PERPLEXITY OF PERTURBATIONS," 2016.
[64] S. A. Sandford, L. J. Allamandola, A. G. G. M. Tielens, K. Sellgren, M. Tapia, and Y. Pendleton, "The interstellar C-H stretching band near 3.4 microns - Constraints on the composition of organic material in the diffuse interstellar medium," Astrophys. J., 1991.
[65] H. Yamazaki et al., "The Influence of Fluorinated Silicon Nitride Gate Insulator on Positive Bias Stability toward Highly Reliable Amorphous InGaZnO Thin-Film Transistors," ECS J. Solid State Sci. Technol., 2014.
[66] T. Ito, Y. Kato, and A. Hiraki, "Hydrogen Bonding onto Microcrystalline Surfaces within Anodized Porous Silicon Crystals Studied by Infrared Spectroscopy,", The Structure of Surfaces II, 1988, pp. 378-383.
[67] S. Kalem, "Synthesis of ammonium silicon fluoride cryptocrystals on silicon by dry etching," Appl. Surf. Sci., 2004.
[68] Hari Singh Nalwa, Silicon-Based Material and Devices, Two-Volume Set,Materials and Processing, Properties and Devices-Elsevier Science, 2001.
[69] P. J. Launer and B. Arkles, "Infrared Analysis of Orgaonsilicon Compounds," Silicon Compd. Silanes Silicones (3rd Ed.), 2013.
[70] Chanda, M., Plastics Technology Handbook, Fifth Edition. Milton: CRC Press, 2017.
[71] George Wypych, "Solvents Use In Various Industries," Handbook of Solvents, vol. 2, 3rd Edition, 2019, ch. 14, pp. 941–942.
[72] Jerry March, Advanced organic chemistry: Reactions, mechanisms and structure, 4th Ed. J. Wiley and Sons, 1992: New York.
[73] J. K. Fink, "Reactive Extrusion," Reactive Polymers: Fundamentals and Applications, 2018, pp. 325–344.
[74] L. A. Felton and J. W. McGinity, "Adhesion of polymeric films to pharmaceutical solids," European Journal of Pharmaceutics and Biopharmaceutics. 1999, 47: 3–14.
[75] G. Molero and H. J. Sue, "Scratch behavior of model epoxy resins with different crosslinking densities," Mater. Des., 2019.
[76] C. Wei, G. Wang, M. Cridland, D. L. Olson, and S. Liu, "Corrosion protection of ships," in Handbook of Environmental Degradation Of Materials: Third Edition, 2018, pp. 533–557.